J. Fluid Mech. (1978), *vol.* 84, *part* 3, *pp.* 471–495
Printed in Great Britain

A theoretical study of the effects of wall conductivity, non-uniform magnetic fields and variable-area ducts on liquid-metal flows at high Hartmann number

By RICHARD J. HOLROYD
Department of Engineering, University of Cambridge
AND JOHN S. WALKER
Department of Theoretical and Applied Mechanics, University of Illinois, Urbana

(Received 12 March 1977)

Flows of incompressible, electrically conducting liquids along ducts with electrically insulating or weakly conducting walls situated in a strong magnetic field are analysed. Except over a short length along the duct where the magnetic field strength and/or the duct cross-sectional area vary, the duct is assumed to be straight and the field to be uniform and aligned at right angles to the duct. Magnitudes of the field strength B_0 and the mean velocity V are taken to be such that the Hartmann number $M \gg 1$, the interaction parameter N $(= M^2/Re) \gg 1$ (Re being the Reynolds number of the flow) and the magnetic Reynolds number $R_m \ll 1$.

For an $O(1)$ change in the product VB_0 along the duct across the non-uniform region, it is shown that:

(i) In the non-uniform region the streamlines and current flow lines follow surfaces containing the field lines satisfying $\int B^{-1} ds =$ constant, the integration being carried out along the field line within the duct; these surfaces are equipotentials and isobarics. This leads to

(ii) a tube of stagnant, but not current-free fluid at the centre of the duct parallel to the field lines around which the flow divides to bypass it. To accommodate this flow,

(iii) the usual uniform field/straight duct flow is disturbed over very large distances upstream and downstream of this region, the maximum length O(duct radius $\times M^{\frac{1}{2}}$) occurring in a non-conducting duct;

(iv) a large pressure drop is introduced into the pressure distribution regardless of the direction of the flow, the effect being most severe in a non-conducting duct, where the drop is O(duct radius $\times$ (uniform field/straight duct pressure gradient) $\times M^{\frac{1}{2}}$);

(v) in the part of the duct with the lower value of VB_0 a region of reverse flow occurs near the centre of the duct and the stagnant fluid.

1. Introduction

The main aim of this paper is to examine theoretically the effects of non-uniform magnetic fields and electrical conductance of the pipe walls on the steady flow of a conducting liquid along a uniform-bore duct when both the Hartmann number M and the interaction parameter N are very large, so that the flow is effectively inviscid and inertialess, and when the magnetic Reynolds number $R_m \ll 1$. It may be regarded, therefore, as complementing analyses by Walker & Ludford (1974*a*, 1975) of the flow

along two semi-infinite circular pipes of different radii connected by an expansion when the pipe wall is non-conducting and weakly conducting (hereafter referred to as thin-walled) respectively. [Henceforth these papers will be referred to as W & L (1974 *a*) and W & L (1975).] In fact, in regions of non-uniform field and/or varying duct cross-section in these types of duct, the streamlines of the flow follow equipotential surfaces containing the magnetic field lines satisfying $\int B^{-1} ds = \text{constant}$, the integration being carried out along the field lines inside the duct. This is a powerful result which allows at least the approximate motion of the fluid to be deduced quickly for a wide range of situations. The current-density streamlines also lie on these surfaces, which are therefore also isobaric surfaces.

Unfortunately, such general results cannot be deduced for the flow in a duct with highly conducting walls. Walker & Ludford (1974*b*) examined the flow in such a duct of variable cross-section situated in a uniform field. The present authors hope to treat the complementary problem of the flow along a uniform-bore duct situated in a non-uniform magnetic field in a subsequent paper.

The emphasis on inertialess flows stems from a report by Hunt & Hancox (1971), in which they estimate the pressure drops in the liquid-metal heat-transfer circuit, part of which lies in regions of intense magnetic field, of a proposed design for a nuclear fusion reactor. Typical values of M and N are quoted as $O(10^4)$, indicating that viscous and inertia forces will indeed be negligible compared with electromagnetic forces. They point out, though, that data on such flows, particularly in thin-walled ducts, are scarce. The relevance of this work, together with work by Holroyd (1976), Walker and co-authors (previously cited literature and the references therein) and several other authors, in fusion-reactor technology has recently been examined by Hunt & Holroyd (1977).

In common with all duct flow analyses at high M, it will be assumed that the flow can be subdivided into an inviscid core region surrounded by Hartmann layers adjacent to walls having a significant normal component of flux density and singular regions at places where Hartmann layers cannot exist (e.g. where the magnetic field lines are tangential to the duct wall). For analytical purposes, it will be assumed that the flow in these singular regions does not significantly affect the core flow.

The relevant equations and boundary conditions for the analysis are set out in §2. In §3 the flow in a non-conducting variable-area duct situated in a non-uniform magnetic field is examined with particular attention focused on the case of a straight circular pipe and a non-uniform field which consists of uniform transverse fields of different strengths upstream and downstream. It is shown that the flow behaves, qualitatively, in a similar manner to the flow in Walker & Ludford's corresponding problem. In the region of non-uniform field (or variable duct area) the flow divides to bypass a tube of stagnant fluid parallel to the field lines which forms around the centre of the duct. To accommodate this flow, the flow that normally exists when the field is uniform and the duct is straight is realized only at very large distances (of order duct radius $\times M^{\frac{1}{2}}$) upstream *and* downstream of the non-uniform region. A pair of trapped eddies forms near the stagnant fluid in the region of weaker uniform field (or larger duct cross-section). Their presence is intimately connected with a current flow along the duct which also introduces a pressure drop of order duct radius $\times$ (uniform field/straight duct) pressure gradient $\times M^{\frac{1}{2}}$.

In §4 the corresponding flow in a duct with very thin conducting walls (a thin-walled

duct) is considered. It turns out to be similar to that in the non-conducting duct but the flow is disturbed over a shorter distance and the pressure drop is smaller relative to the usual pressure gradients.

Finally, in § 5 limitations of the analysis and some of its none-too-obvious applications are mentioned. The effects of increasing the wall conductivity are discussed and some comparisons are made with flows in which inertial effects are present.

2. Governing equations and boundary conditions

The derivation of the equations governing the steady motion of an isotropic, electrically conducting, incompressible liquid in the presence of a steady magnetic field $\mathbf{B}^*$ when the magnetic Reynolds number $R_m = \mu\sigma V a \ll 1$ may be found in several texts, e.g. Shercliff (1965, chap. 2); they are

$$\rho\mathbf{v}^*.\nabla\mathbf{v}^* = -\nabla p + \mathbf{j}^* \wedge \mathbf{B}^* + \eta\nabla^2\mathbf{v}^*, \quad \mathbf{j}^* = \sigma(-\nabla\phi^* + \mathbf{v}^* \wedge \mathbf{B}^*), \tag{2.1a,b}$$

$$\nabla.\mathbf{v}^* = \nabla.\mathbf{j}^* = \nabla.\mathbf{B}^* = 0, \quad \nabla \wedge \mathbf{B}^* = 0, \tag{2.1c–f}$$

where $\mathbf{v}^*$, p, $\mathbf{j}^*$ and ϕ^* represent the velocity, pressure, electric-current density and electric potential respectively and ρ, σ, η and μ are respectively the fluid properties density, electrical conductivity, viscosity and permeability.

For the following analysis (2.1*a–f*) will be expressed in non-dimensional form in terms of ρ, σ, η, the mean velocity of the flow V, the hydraulic radius of the pipe a and the maximum uniform flux density B_0 of the applied magnetic field:

$$N^{-1}\mathbf{v}.\nabla\mathbf{v} = -\nabla h + \mathbf{j} \wedge \mathbf{B} + M^{-2}\nabla^2\mathbf{v}, \quad \mathbf{j} = -\nabla\phi + \mathbf{v} \wedge \mathbf{B}, \tag{2.2a,b}$$

$$\nabla.\mathbf{v} = \nabla.\mathbf{j} = \nabla.\mathbf{B} = 0, \quad \nabla \wedge \mathbf{B} = 0, \tag{2.2c–f}$$

where $\mathbf{v} = \mathbf{v}^*/V$, $\mathbf{B} = \mathbf{B}^*/B_0$, $\mathbf{j} = \mathbf{j}^*/\sigma V B_0$, $\phi = \phi^*/aVB_0$† and $h = p/\rho V^2 N$. Here $M = aB_0(\sigma/\eta)^{\frac{1}{2}}$ is the Hartmann number and $N = \sigma B^2 a/\rho V$ is the interaction parameter.

At this stage it will be assumed that M and N are sufficiently large for viscous and inertial effects to be ignored, so that (2.2*a*) reduces to

$$\nabla h = \mathbf{j} \wedge \mathbf{B}, \tag{2.3}$$

but additional constraints will be placed on them later (§ 5.1). An important implication of this approximation is that all the governing equations of the flow (2.2*b–f*) and (2.3) are now linear and hence the fluid and current flows are reversible. For convenience the uniform magnetic fields will be taken to be directed along the y axis and the fluid will move in the direction in which the product VB_0 decreases, this also being the direction of the x axis.

For all types of duct the boundary condition on velocity at the boundary of the core flow, neglecting $O(M^{-1})$ terms, is

$$v_n = 0, \tag{2.4a}$$

where $\hat{\mathbf{n}}$ denotes the unit normal to the wall directed into the fluid. The electrical boundary conditions depend on the type of duct; at a non-conducting wall Hunt &

† Walker & Ludford define their electric potential as minus that defined here. The present terminology is consistent with the usual definition of the strength of an irrotational electric field as $-\nabla\phi^*$.

Ludford (1968) showed that the normal components of current density and vorticity are related by

$$j_n = \text{sgn}\,(\hat{\mathbf{n}}.\mathbf{B})\, M^{-1}(\nabla \wedge \mathbf{v})_n, \tag{2.4b}$$

whilst at a thin wall it may be shown that

$$j_n = \text{sgn}\,(\hat{\mathbf{n}}.\mathbf{B})\, \Phi \nabla^2 \phi, \tag{2.4c}$$

where Φ = (electrical conductivity of wall) × (wall thickness)/σa is the conductance ratio and lies in the range $1 \gg \Phi \gg M^{-1}$ and the Laplacian operator does not contain the derivative $\partial^2/\partial n^2$.

3. The core flow in a non-conducting duct

3.1. *Longitudinal subdivisions of the flow*

Since it is assumed that far upstream and downstream both the field strength B_y and the duct cross-section are constant, the flow eventually realized far from the non-uniform region will be that deduced by Shercliff (1956) (hereafter referred to as the fully developed flow), in which the core flow variables j_z and h are $O(M^{-1})$ and v_x and ϕ are $O(1)$ (the axes being those defined above). To a good approximation the z component of (2.2b) may be written as $d\phi/dz = v_x B_y$, so, should there be an $O(1)$ change in field strength or duct cross-section and hence mean velocity along the duct, then there will also be an $O(1)$ change in potential, which in turn suggests a longitudinal current flow j_x. Equation (2.2d) implies that, to match the $O(M^{-1})$ transverse current, j_x must be $O(l/M)$, where l is the distance over which j_x exists, whereas (2.2b) implies that j_x is $O(1/l)$. These two results can be reconciled only if $l = O(M^{\frac{1}{2}})$, so that $j_x = O(M^{-\frac{1}{2}})$.

So far the length over which the field strength or duct area changes has not been specified. Three possibilities come to mind:

(i) an $O(1)$ length, in which case the longitudinal current flow could extend for $O(M^{\frac{1}{2}})$ distances upstream and downstream of the non-uniform field region,

(ii) an $O(M^{\frac{1}{2}})$ length, so that the longitudinal current flow is largely confined to the non-uniform region,

(iii) an $O(M)$ length.

In this paper only case (i) will be considered because then the fully developed flow is most severely disturbed; as the length of the non-uniform region increases the effects on the flow are attenuated.

Tentatively, then, the flow is subdivided into three sections, namely a region of length $O(1)$ where the field strength and/or the duct area vary flanked by regions of length $O(M^{\frac{1}{2}})$ upstream and downstream where the field strength and duct area are uniform but where the flow may not be fully developed. In the former region (2.2b) demands that the current densities are $O(M^{-\frac{1}{2}})$ but in the long regions only the longitudinal current-density component is $O(M^{-\frac{1}{2}})$, the other components being $O(M^{-1})$. The velocity is assumed to be $O(1)$ throughout.

3.2. *Analysis of the flow in the* $O(1)$ *length non-uniform region*

Since the current density here is $O(M^{-\frac{1}{2}})$, (2.2b) may be written as

$$\nabla\phi = \mathbf{v} \wedge \mathbf{B} + O(M^{-\frac{1}{2}}) + \ldots, \tag{3.1}$$

which suggests that the fluid behaves as if it were perfectly conducting (Shercliff 1965, §3.4). It follows that the magnetic analogies of the Kelvin and Helmholtz theorems about vorticity and circulation may be used to show that (i) the area $\delta\mathbf{A}$ enclosed by a loop of fluid particles moving with the flow will vary such that

$$\mathbf{B}.\delta\mathbf{A} = \text{constant} \tag{3.2}$$

and (ii) a line of fluid particles initially aligned along a magnetic field line will remain so. Now for any tube of elemental cross-sectional area $\delta A(s)$ in the fluid whose surface generators are coincident with magnetic field lines

$$\int \delta\mathbf{A}(s).d\mathbf{s} = \text{constant},$$

where s is the distance measured along a field line and the integration is carried out along field lines inside the duct. Combining this with (3.2) yields the following important result: *the streamlines lie on surfaces containing all the field lines satisfying*

$$\int B^{-1}\,ds = \text{constant}. \tag{3.3}$$

Furthermore, (3.1) implies that these are equipotential surfaces since ϕ can vary only in the direction perpendicular to both the streamlines and the field lines. Equation (3.3) is a completely general result but note that the velocity distribution over the surface is not uniquely determined: it depends on the flow upstream and downstream of the non-uniform region. A formal mathematical proof of (3.3) has been derived independently by Kulikovskii (1973).†

A similar result can be derived for the $O(M^{-\frac{1}{2}})$ current flow in this region as follows. Equation (2.3) implies that h may vary only in directions perpendicular to both the current-density streamlines and the field lines. Between two isobaric surfaces on which the pressure is h and $h+\delta h$, continuity of current flow requires

$$\int j_\perp\,\delta n(s)\,ds = \text{constant}, \tag{3.4}$$

where $j_\perp$ is the component of current density normal to the field lines, and, by definition, tangential to the isobaric surfaces $\delta n(s)$ is the distance between the isobaric surfaces (which varies along the field lines) and the integration is carried out along field lines inside the duct. The current flow normal to the duct wall at the edge of the core, necessary to satisfy boundary condition (2.4*b*), can be neglected since it is only $O(M^{-1})$. Although $\delta n(s)$ varies, $\delta h = j_\perp B\,\delta n(s)$ does not and so (3.4) may be rewritten as

$$\delta h \int B^{-1}\,ds = \text{constant}.$$

Thus the current flow is also along the surfaces defined by (3.3) and they are now isobaric surfaces. In passing, it may be noted that this method can also be used to derive the former result for the fluid motion.

† He also derives an expression for the pressure drop along the duct by assuming that the currents are $O(M^{-1})$ rather than $O(M^{-\frac{1}{2}})$. Consequently he does not derive the other result derived here for the current flow along the surfaces defined by (3.3). Surprisingly, he does not point out that his solutions do not show how the fluid is distributed on the surfaces.

This last result was derived mathematically for the special case of a uniform field by Hunt & Ludford (1968). Upon putting $\mathbf{j} \equiv 0$, or more generally $|\mathbf{j}| \ll |\mathbf{v}|$, they then derived (3.3), again for the uniform field case.

3.3. *Analysis of the flow in the $O(M^{\frac{1}{2}})$ length regions*

In these regions, upstream and downstream of the non-uniform region, the field strength and duct cross-section are taken as constant. Shercliff's fully developed flow is not realized in the immediate vicinity of the non-uniform region but there is a gradual transition to it over an $O(M^{\frac{1}{2}})$ length. This flow may be analysed in the same manner as in W & L (1974*a*), namely by compressing the x scale by defining $X = xM^{-\frac{1}{2}}$ and then expressing the core variables as power series in $M^{-\frac{1}{2}}$ and selecting the leading terms (e.g. $\mathbf{j} = \mathbf{j}^{(0)} + \mathbf{j}^{(\frac{1}{2})}M^{-\frac{1}{2}} + \mathbf{j}^{(1)}M^{-1} + \ldots$ and $\mathbf{j}^{(0)} = 0$, leaving $\mathbf{j}^{(\frac{1}{2})}$ as the leading term). The governing equations for the flow will be derived for an arbitrarily shaped duct of uniform cross-section but, because a general solution is not possible, their solution for a circular duct of radius R will be given, this being the most useful shape from a practical point of view.

From (2.2*b*) and (2.3) it follows that $\partial\phi^{(0)}/\partial y = \partial h^{(\frac{1}{2})}/\partial y = 0$ so both $\phi^{(0)}$ and $h^{(\frac{1}{2})}$ are functions of X and z only. The same equations may now be used to show that

$$j_x^{(\frac{1}{2})} = \frac{1}{B_y}\frac{\partial h^{(\frac{1}{2})}}{\partial z}, \quad j_y^{(1)} = P(X,z), \quad j_z^{(1)} = -\frac{1}{B_y}\frac{\partial h^{(\frac{1}{2})}}{\partial X}, \tag{3.5a–c}$$

$$v_x^{(0)} = \frac{1}{B_y}\frac{\partial \phi^{(0)}}{\partial z}, \quad v_y^{(\frac{1}{2})} = \frac{1}{B_y^2}\left\{y\frac{\partial^2 h^{(\frac{1}{2})}}{\partial z^2} + Q(X,z)\right\}, \quad v_z^{(\frac{1}{2})} = -\frac{1}{B_y^2}\frac{\partial h^{(\frac{1}{2})}}{\partial z} - \frac{1}{B_y}\frac{\partial \phi^{(0)}}{\partial X}, \tag{3.6a–c}$$

where $B_y \leqslant 1$ is the (uniform) field strength and $P(X,z)$ and $Q(X,z)$ are functions of integration which are zero for a symmetric duct. Boundary conditions (2.4*a*, *b*) may now be written as

$$v_y^{(\frac{1}{2})} - v_z^{(\frac{1}{2})}f' = 0, \quad j_y^{(1)} - j_z^{(1)}f' = -\partial v_x^{(0)}/\partial z \tag{3.7a, b}$$

respectively, where $y = f(z)$ represents either the upper or the lower wall of the duct, and after substituting (3.5*a–c*) and (3.6*a–c*) into (3.7*a*, *b*) it may be shown that $h^{(\frac{1}{2})}$ and $\phi^{(0)}$ satisfy

$$\frac{\partial}{\partial z}\left(g(z)\frac{\partial h^{(\frac{1}{2})}}{\partial z}\right) + B_y g'\frac{\partial \phi^{(0)}}{\partial X} = 0, \quad \frac{\partial^2 \phi^{(0)}}{\partial z^2} + \tfrac{1}{2}g'\frac{\partial h^{(\frac{1}{2})}}{\partial X} = 0,$$

where $g(z)$ is the local height of the duct.

For a circular duct of radius R, $g = 2(R^2 - z^2)^{\frac{1}{2}}$ and these equations become

$$(R^2-z^2)\frac{\partial^2 h^{(\frac{1}{2})}}{\partial z^2} - z\left(\frac{\partial h^{(\frac{1}{2})}}{\partial z} + B_y\frac{\partial \phi^{(0)}}{\partial X}\right) = 0, \quad (R^2-z^2)^{\frac{1}{2}}\frac{\partial^2 \phi^{(0)}}{\partial z^2} - z\frac{\partial h^{(\frac{1}{2})}}{\partial X} = 0. \tag{3.8a, b}$$

Solutions to these equations must satisfy the symmetry conditions

$$\phi^{(0)} = \partial h^{(\frac{1}{2})}/\partial z = 0 \quad \text{at} \quad z = 0 \tag{3.9a, b}$$

and approach the fully developed flow solutions as $|X| \to \infty$, namely

$$\phi^{(0)} \to \frac{3\pi}{16}\frac{B_y}{R}\left(R^2 \arcsin\frac{z}{R} + z(R^2-z^2)^{\frac{1}{2}}\right), \quad h^{(\frac{1}{2})} \to -\frac{3\pi}{8}\frac{B_y}{R}X + k, \tag{3.9c, d}$$

where k is a constant whose value in the upstream pipe will be taken as zero. In addition they must satisfy the singularity conditions

$$\partial\phi^{(0)}/\partial z \to 0, \quad (R^2-z^2)\,\partial^2 h^{(\frac{1}{2})}/\partial z^2 \to 0 \quad \text{as} \quad |z| \to R \tag{3.9e,f}$$

near the singular regions at $|z| = R$.

Taking $R = B_y = 1$, $X < 0$ in the upstream pipe and $R = 1$, $0 < B_y < 1$, $X > 0$ in the downstream pipe, (3.3) implies that the flow must divide at the plane $z = 0$ as it leaves the upstream pipe and move towards those walls of the pipe at which the field lines are tangential. Between the two halves of the divided main flow is left a volume of stagnant fluid, this being the only 'flow' that is symmetric about the plane $z = 0$ and has streamlines on the equipotential surfaces defined by (3.3) (which would imply antisymmetric flow about the plane $z = 0$). Thus the upstream flow at $X = 0^-$ and the downstream flow at $X = 0^+$ are not continuous, but the solutions for each flow must satisfy the following matching conditions:

$$\left.\begin{aligned} \phi^{(0)}(0^+, z) &= \phi^{(0)}(0^-, Z) \\ h^{(\frac{1}{2})}(0^+, z) &= h^{(\frac{1}{2})}(0^-, Z) \end{aligned}\right\} \quad \text{for} \quad (R^2-B_y^2)^{\frac{1}{2}} < |z| < R, \tag{3.9g,h}$$

$$\phi^{(0)}(0^+, z) = 0 \quad \text{for} \quad |z| < (R^2-B_y^2)^{\frac{1}{2}}, \tag{3.9i}$$

where

$$Z = \{1 - B_y^{-2}(R^2-z^2)\}^{\frac{1}{2}}. \tag{3.9j}$$

Equations (3.9g,h) represent matching of the streamlines and current flow lines and (3.9i) follows from the fact that v_x and hence $\partial\phi^{(0)}/\partial z$ is zero in the range of z indicated.

3.4. *Numerics*

The numerical analysis for the regions of length $O(M^{\frac{1}{2}})$ upstream and downstream of the non-uniform field region closely parallels the analysis given by W & L (1974a) for similar regions in non-conducting pipes upstream and downstream of a non-conducting expansion or contraction. Solutions to (3.8a,b) may be obtained by separation of variables; writing

$$\phi^{(0)} = -(B_y R)^{\frac{1}{2}}\,\Phi(\xi)\exp(-\lambda X R^{-\frac{3}{2}} B_y^{-\frac{1}{2}}), \tag{3.10a}$$

$$h^{(\frac{1}{2})} = B_y H(\xi)\exp(-\lambda X R^{-\frac{3}{2}} B_y^{-\frac{1}{2}}), \tag{3.10b}$$

where

$$\xi = (1-z/R)^{\frac{1}{2}}, \tag{3.10c}$$

results in an eigenvalue problem consisting of the pair of ordinary differential equations

$$\left.\begin{aligned} (2-\xi^2)H'' - \xi H' &= 4\lambda(1-\xi^2)\,\Phi \\ (2-\xi^2)^{\frac{1}{2}}(\xi\Phi'' - \Phi') &= 4\lambda\xi^2(1-\xi^2)H \end{aligned}\right\} \quad \text{in} \quad 0 < \xi < 1 \tag{3.11a,b}$$

together with the conditions

$$H'' - \xi^{-1}H' \to 0, \quad \xi^{-1}\Phi' \to 0 \quad \text{as} \quad \xi \to 0 \tag{3.12a,b}$$

and

$$\Phi = H' = 0 \quad \text{at} \quad \xi = 1. \tag{3.12c,d}$$

Since the constants R and B_y have now disappeared, the eigenvalues and eigenfunctions apply to both the upstream and the downstream region of length $O(M^{\frac{1}{2}})$. In fact they apply to a circular non-conducting pipe of any diameter and with any uniform transverse magnetic field, including the pipes in the problem treated by W & L (1974a).

Equations (3.11) and (3.12) are identical to equations (12) and (13) in W & L (1974*a*), so that the first sixty positive eigenvalues for the present problem are those given in table 1 in W & L (1974*a*) while the eigenfunctions can be generated in the manner described in W & L (1974*a*).

The solutions in the upstream and downstream regions of length $O(M^{\frac{1}{2}})$ are now approximated by truncated eigenfunction expansions. The eigenvalues occur in pairs $\lambda_{\pm j}$ ($j = 1, 2, 3, \ldots$), where $\lambda_{-j} = -\lambda_j < 0$, $H_{-j} = H_j$ and $\Phi_{-j} = -\Phi_j$. The exception is $\lambda_0 = 0$, which is a double eigenvalue corresponding to fully developed flow (3.9*c*, *d*). Positive eigenvalues λ_j are excluded in the upstream eigenfunction expansions and negative eigenvalues λ_{-j} are excluded in the downstream expansions, because they make ϕ and h unbounded as $X \to \mp\infty$ respectively. Since $R = B_y = 1$ for the upstream region, its eigenfunction expansions are

$$h^{(\frac{1}{2})} = -\tfrac{3}{8}\pi X + \sum_{j=1}^{60} a_j H_j \exp(\lambda_j X), \tag{3.13a}$$

$$\phi^{(0)} = \tfrac{3}{16}\pi[\arcsin z + z(1-z^2)^{\frac{1}{2}}] + \sum_{j=1}^{60} a_j \Phi_j \exp(\lambda_j X), \tag{3.13b}$$

and, since $R = 1$ for the downstream region, its eigenfunction expansions are

$$h^{(\frac{1}{2})} = -\tfrac{3}{8}\pi B_y^2 X + k + B_y \sum_{j=1}^{60} b_j H_j \exp(-\lambda_j X B_y^{-\frac{1}{2}}), \tag{3.13c}$$

$$\phi^{(0)} = \tfrac{3}{16}\pi B_y[\arcsin z + z(1-z^2)^{\frac{1}{2}}] - B_y^{\frac{1}{2}} \sum_{j=1}^{60} b_j \Phi_j \exp(-\lambda_j X B_y^{-\frac{1}{2}}). \tag{3.13d}$$

The 121 unknown coefficients a_j, k and b_j in these expansions are now determined by satisfying the matching conditions (3.9*g–i*) in a least-mean-square sense. The integral of the squares of the errors for these conditions is

$$I = \int_0^{\Xi} \{[\phi^{(0)}(0^+, z) - \phi^{(0)}(0^-, Z)]^2 + [h^{(\frac{1}{2})}(0^+, z) - h^{(\frac{1}{2})}(0^-, Z)]^2\} d\xi + \int_{\Xi}^1 [\phi^{(0)}(0^+, z)]^2 d\xi, \tag{3.14a}$$

where z is given as a function of ξ by (3.10*c*), Z is given as a function of z by (3.9*j*), while

$$\Xi = \left[1 - \left(1 - \frac{B_y^2}{R^2}\right)^{\frac{1}{2}}\right]^{\frac{1}{2}}. \tag{3.14b}$$

The minimum over the functions (3.13) is given by

$$\partial I/\partial a_j = \partial I/\partial k = \partial I/\partial b_j = 0 \quad \text{for} \quad j = 1, 2, \ldots, 60, \tag{3.14c}$$

which are 121 linear equations for the 121 unknown coefficients. Simpson's rule is used to evaluate the integrals of products of eigenfunctions which appear as coefficients in (3.14*c*) with a step of 0·001 in ξ except on each side of Ξ, where smaller, irregular steps are used. Once equations (3.14*c*) have been solved, the expansions (3.13) give $h^{(\frac{1}{2})}$ and $\phi^{(0)}$ in the two regions of length $O(M^{\frac{1}{2}})$ and (3.4) and (3.5) give the other variables.

Equations (3.14*c*) have been solved for the 121 coefficients for $B_y = 0{\cdot}1, 0{\cdot}2, 0{\cdot}3, \ldots, 0{\cdot}9$, and special attention is focused on the coefficient k, whose physical meaning will be discussed in the next subsection. In addition, for $B_y = 0{\cdot}5$ the values of $\phi^{(0)}$, $v_x^{(0)}$, $h^{(\frac{1}{2})}$, $j_x^{(\frac{1}{2})}$ and $j_z^{(1)}$ at various points (X, z) were determined numerically. The results will be presented and discussed in the next subsection.

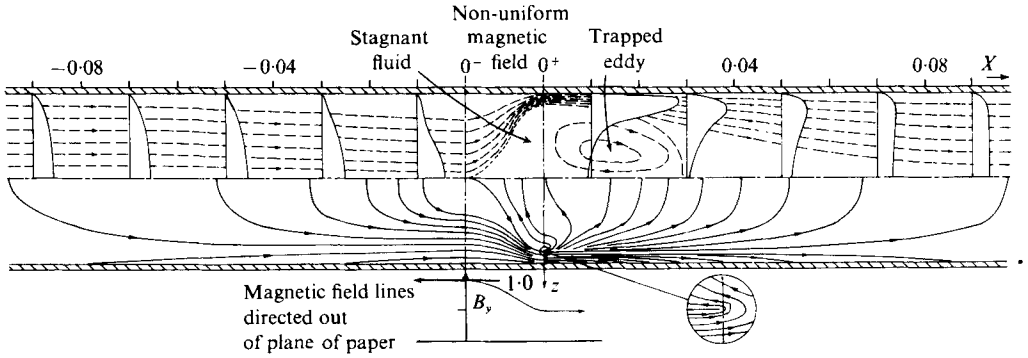

FIGURE 1. Sketch on plane $y = 0$ of current-density flow lines associated with disturbed flow (lower half of diagram) and streamwise velocity profiles and streamlines (upper half of diagram) in a non-conducting duct. Note that the length of the non-uniform field region is exaggerated.

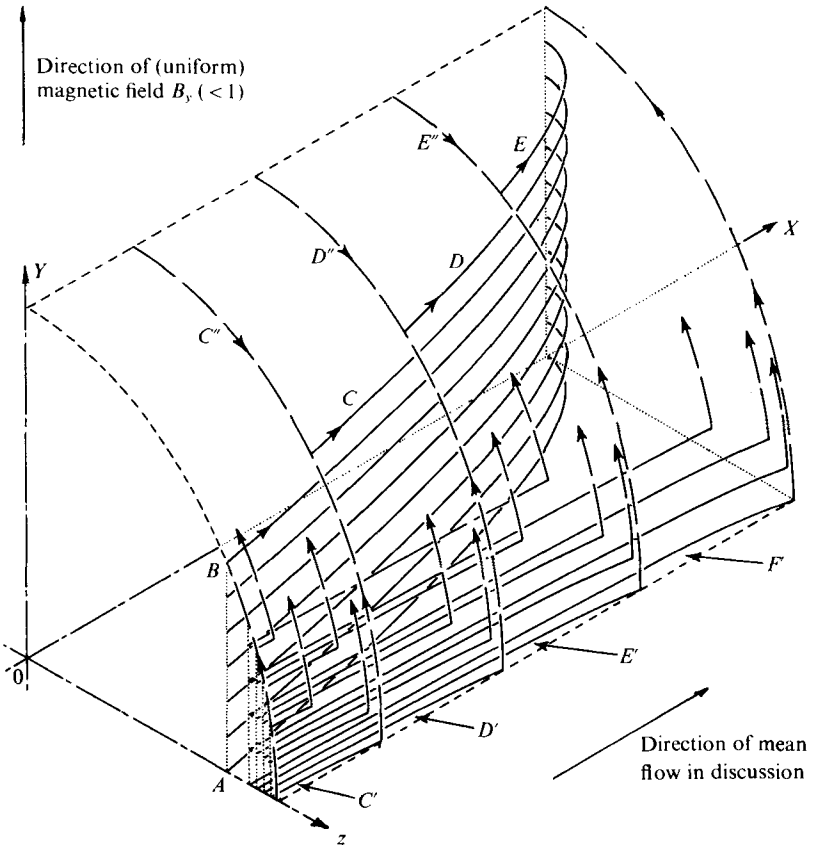

FIGURE 2. Current-density flow lines just downstream of non-uniform field region (i.e. $X > 0$) in a non-conducting duct. ——, core currents; – – –, Hartmann-layer currents.

3.5. *Discussion of computed results for* $B_y = 0{\cdot}5$, $R = 1$

Figure 1 is a cross-section of the circular duct on the plane $y = 0$ showing the streamlines and some velocity profiles of the flow and the current flow lines associated with the disturbed flow. Because the duct is symmetric $j_y \equiv 0$, so it follows from (3.5) and (3.9*d*) that these current flow lines are defined by curves satisfying $h + \frac{3}{8}\pi(B_y/R)X = \text{constant}$ and are independent of y. The complete pattern of current flow lines can be obtained by superposing the flow lines of the $O(M^{-1})$ uniform transverse current flow (the first flow lines then being curves satisfying $h = \text{constant}$).

Upon closer examination the current flow just downstream of the non-uniform field region is as shown in figure 2 (the uniform transverse current component is still omitted) and its behaviour and effect on the flow may be illustrated by reference to the following.

(i) The seven current flow lines between A and B and those labelled C, D and E, which lie vertically above each other and represent current flow in the core on planes $y = \text{constant}$.

(ii) The current flow lines C', D' and E' on the plane $y = 0$, which enter the Hartmann layer via the singular regions at $y = 0$, $z = R$ and later reappear as *part* of the core current flow lines C, D and E respectively. (Also shown are several flow lines directly above C', D' and E' on planes $y = \text{constant}$ (> 0), which enter the Hartmann layer directly, but only the first parts of their paths in the Hartmann layer are shown to avoid confusion.)

(iii) The Hartmann-layer currents C'', D'' and E'', which contribute to the core current flow lines C, D and E respectively.

The Hartmann-layer current due to the uniform $O(M^{-1})$ transverse core current flow is augmented by that entering along current flow lines such as C' in order to satisfy boundary condition (2.4*b*) because of the greatly increased vorticity there since the fluid is moving in a small part of the duct cross-section. However, because this fast-moving fluid does not fill the whole of the duct cross-section, current leaves the Hartmann layer as the vorticity decreases and flows across the core on a plane $y = \text{constant}$. Thus current flow line C', for example, reappears as part of current flow line C. Since the current-density distribution is independent of y, further current flows into flow line C from C'' in the Hartmann layer to ensure that the current-density variation along flow line C is the same as that along those between A and B. Significantly, the Hartmann-layer currents C'', D'' and E'' flow in a direction corresponding to reverse flow in the core, thus giving rise to the trapped eddies.

A further consequence of the current flow follows from the x component of (2.3), namely $dh/dx = j_z B_y$, where h and j_z are here associated with only the disturbance current flow. Integrating this equation over the whole length of the duct gives the following result:

$$\Delta h = \int_{-\infty}^{\infty} \frac{dh}{dx}\,dx = \underbrace{\int_{-\infty}^{0} j_z\,dx}_{\text{upstream}} + B_y \underbrace{\int_{0}^{\infty} j_z\,dx}_{\text{downstream}}$$

(the contribution of the current in the non-uniform field region is $O(M^{-1})$ and its neglect will be justified below). Now, at the downstream end of the non-uniform field region the total current flow from (or to) upstream lies between the planes $y = \pm B_y$, but on continuing downstream some of this current is redistributed to those parts

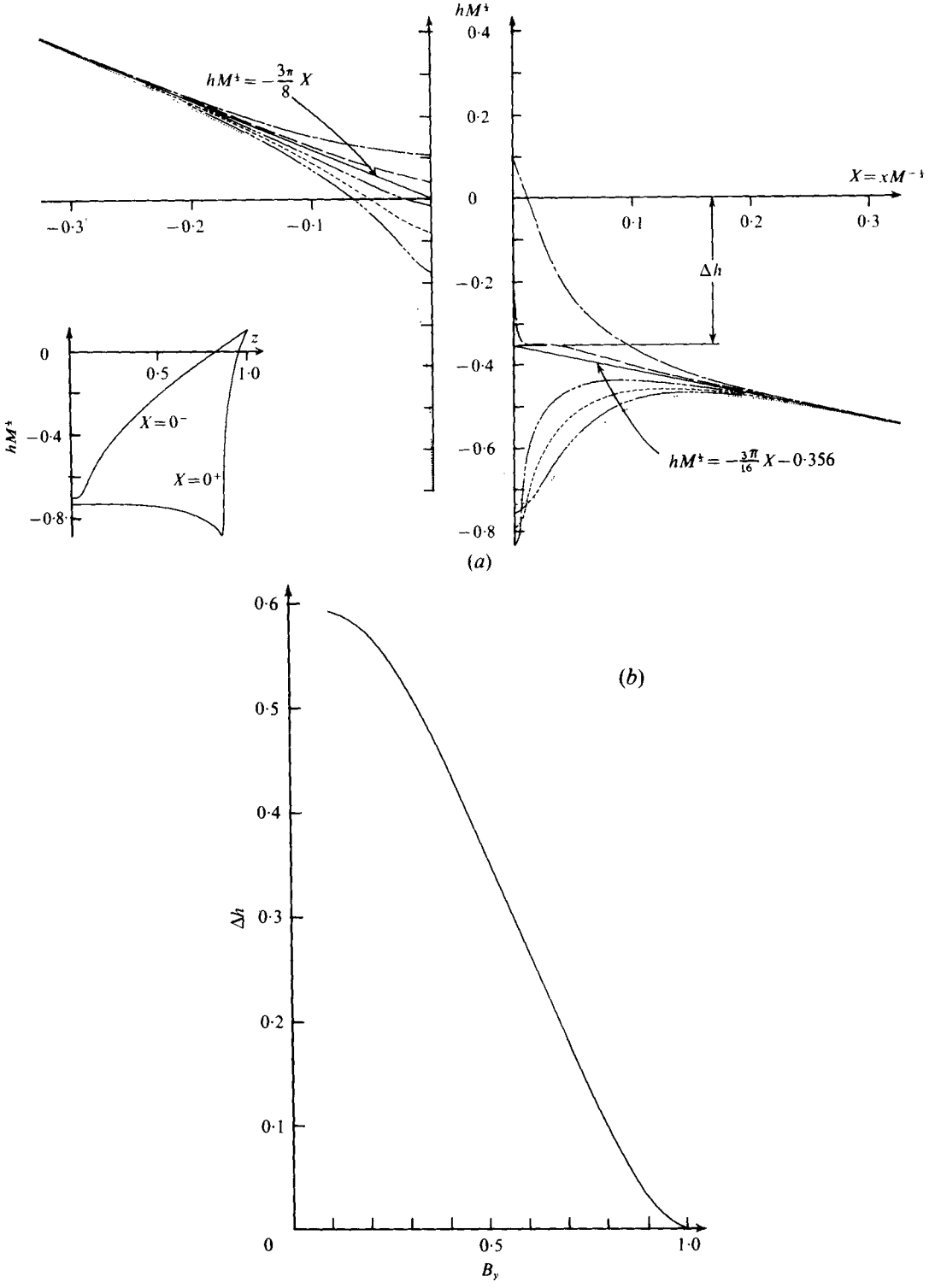

FIGURE 3. (*a*) Pressure distribution along a non-conducting duct on the plane $y = 0$. – – –, $z = 1$; ——, $z = 0{\cdot}9$; —·—·—, $z = 0{\cdot}8$; – – –, $z = 0{\cdot}7$; —·—·—·—, $z = 0{\cdot}55$; · · · · ·, $0 \leqslant z \leqslant 0{\cdot}3$. (*b*) Variation of the pressure drop Δh in a non-conducting duct with B_y.

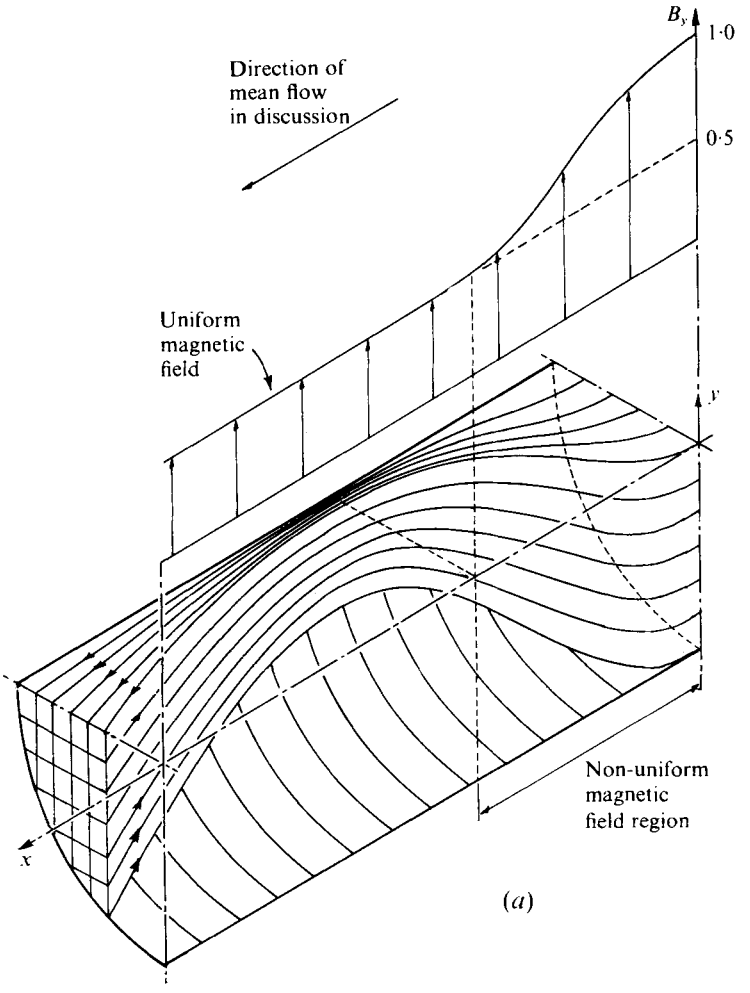

FIGURE 4 (*a*). For legend see opposite.

of the duct above and below these planes via the Hartmann layer (e.g. flow lines C', D' and E' in figure 2). Since $j_z > 0$ upstream of the non-uniform field region and $j_z < 0$ downstream of it,

$$\int_{-\infty}^{0} j_z dx \geqslant -B_y \int_{0}^{\infty} j_z dx$$

upstream downstream

and hence $\Delta h > 0$. In fact, since $j_z = O(M^{-1})$ and flows over an $O(M^{\frac{1}{2}})$ length, then $\Delta h = O(M^{-1}) \times O(M^{\frac{1}{2}}) = O(M^{-\frac{1}{2}})$ (thereby justifying the neglect of the $O(M^{-1})$ current in the non-uniform field region). In other words, the current flow associated with the disturbed flow gives rise to a pressure drop Δh of $O(M^{-\frac{1}{2}})$ which is represented by the coefficient k in (3.9*d*) and (3.13*c*) and which can be seen in the computed pressure distribution along the duct in figure 3(*a*).

Figure 3(*b*) shows how the pressure drop varies with B_y in a uniform-bore circular pipe but comments on this graph will be reserved until the flow in the thin-walled duct has been considered. Computations of the pressure-drop variation in a circular pipe

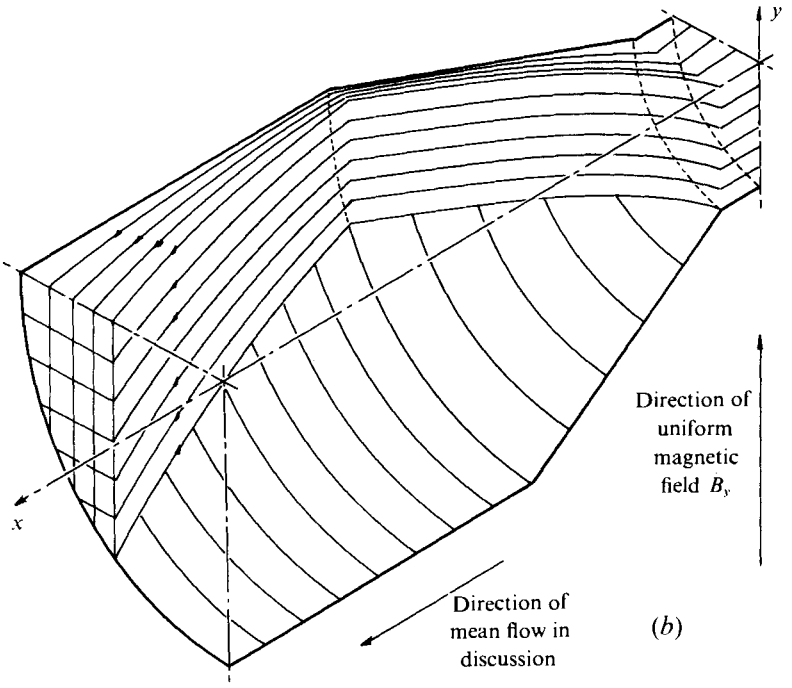

FIGURE 4. (*a*) Sketch of streamlines in, and just downstream of, non-uniform field region in a straight pipe with stagnant fluid and trapped eddies omitted. (*b*) Sketch of streamlines in, and just downstream of, expansion joining two straight pipes of different radii with stagnant fluid and trapped eddies omitted (problem studied by W & L 1974*a*). In the expansion each equipotential surface is of constant height.

with an expansion situated in a uniform field have not been carried out since it seems reasonable to believe that the results would differ only qualitatively from those in figure 3(*b*).

The motion of the fluid in and just downstream of the non-uniform field region is shown in figure 4(*a*), where both the tube of stagnant fluid and the trapped eddies have been omitted and it can be seen how the fluid moves into a smaller part of the cross-section of the duct, thereby increasing its velocity and vorticity. For comparison, and completeness, the corresponding flow in an expansion situated in a uniform field (Walker & Ludford's problem) is shown in figure 4(*b*).

Computed potential and velocity profiles are shown in figures 5 and 6 respectively. A surprising feature of the flow, clearly visible in figure 1, is the increase in the velocity of the fluid at the centre of the duct as it approaches the non-uniform field region. This may be explained by referring to figure 5, which indicates that for $X < 0$ the potential at the wall decreases (for $z > 0$) and consequently the potential gradient $\partial\phi/\partial z$ and hence the streamwise velocity $v_x = B_y^{-1}\,\partial\phi/\partial z$ must also decrease near the wall. To maintain the flow rate along the duct the velocity of the flow near $z = 0$ must increase to compensate for the lower velocities near the walls, and this is reflected in the higher potential gradients near $z = 0$. When $X > 0$ the steepest potential gradients and velocities are found near the wall. These decrease as the potential gradually falls to its

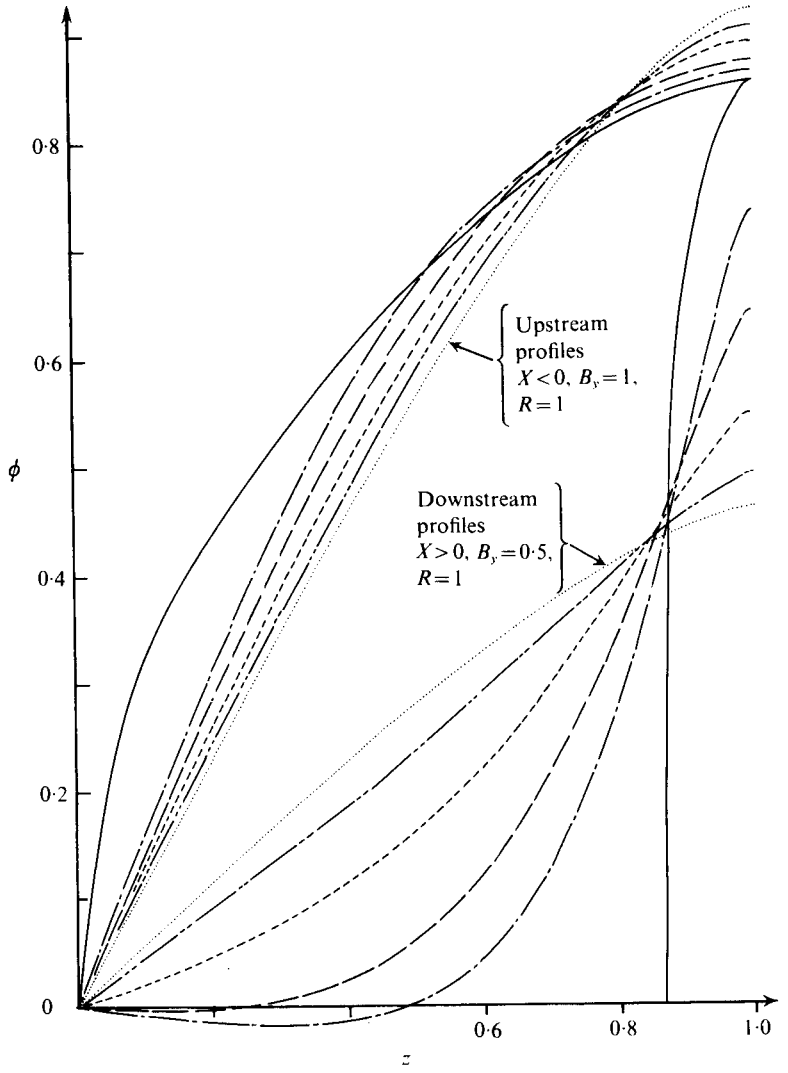

FIGURE 5. Electric potential distribution in a non-conducting duct on the plane $y = 0$. ——, $|X| = 0$; —·—, $|X| = 0{\cdot}01$; ——, $|X| = 0{\cdot}02$; – – –, $|X| = 0{\cdot}04$; —··—, $|X| = 0{\cdot}07$; ·····, $|X| \geqslant 0{\cdot}1$.

downstream fully developed flow value and the fluid velocity must therefore increase at the centre of the duct.

Reversing the direction of the flow reverses the current flow and the rotation of the trapped eddies but leaves the streamline and current flow line patterns unchanged. In addition, there will still be a pressure *drop* of the same magnitude.

3.6. *The extent of the non-uniform region*

A knowledge of the extent of the non-uniform region has not been required in the above analysis and in figure 1 an arbitrary length has been chosen. In fact the length of the non-uniform region can be defined precisely only when the magnetic field is

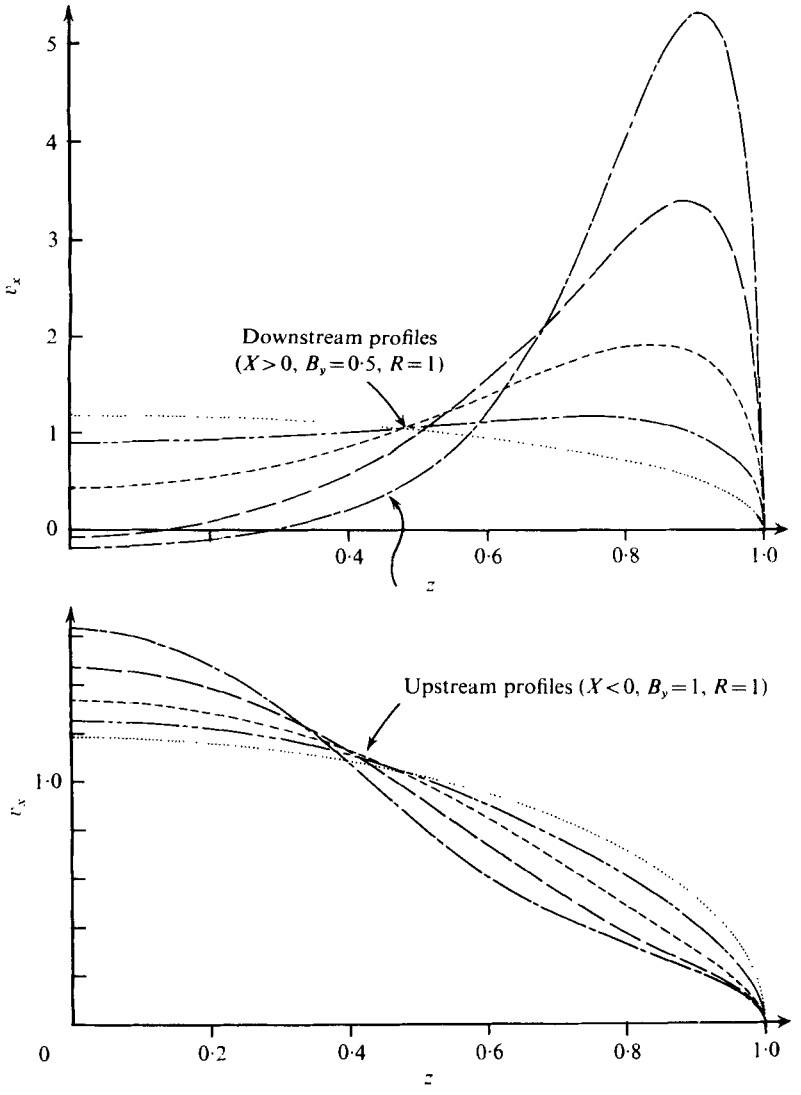

FIGURE 6. Profiles of the velocity component v_x in a non-conducting duct on the plane $y = 0$. Numerical errors preclude computation of profiles at $X = 0^-$ and 0^+. Curves for other values of X as in figure 5.

uniform and the duct comprises two straight pipes of different radii connected by an expansion whose walls have a finite slope in the streamwise direction at each end. In all other cases, especially when non-uniform magnetic fields are involved, the uniform/non-uniform boundary can be defined only in approximate terms as follows.

In the non-uniform region

$$\phi^{(0)} = \phi^{(0)}\left(\int B^{-1}\,ds\right)$$

since the equipotential surfaces are defined by (3.3). If these surfaces are continued into the straight parts of the duct, where the field is uniform, they become planes

parallel to the centre-plane $z = 0$ defined by $g(z)/B_y = \text{constant}$. However, $\partial\phi^{(0)}/\partial x = O(M^{-\frac{1}{2}})$ in these regions whereas in the non-uniform region

$$\frac{\partial\phi^{(0)}}{\partial x} = \phi^{(0)\prime}\frac{\partial}{\partial x}\left\{\int B^{-1}ds\right\} \approx O(1).$$

Since $\phi^{(0)\prime}$ is $O(1)$ a convenient definition of the non-uniform region's boundaries is where

$$\left|\frac{\partial}{\partial x}\int\frac{ds}{B}\right| = M^{-\frac{1}{2}}.$$

Further support for this definition follows from the fact that the analysis required to derive the results in §3.2 and the analysis presented in §3.3 are invalid when

$$|\partial(\int B^{-1}ds)/\partial x| = O(M^{-\frac{1}{2}})$$

(Holroyd 1976, §9.4).

4. The core flow in a thin-walled duct

4.1. *Relationship with the flow in a non-conducting duct*

For analytical purposes, the thin-walled duct will be defined as a duct whose conductance ratio Φ lies in the range

$$M^{-\frac{1}{2}} \ll \Phi^{\frac{1}{2}} \ll 1.$$

This is a more strict condition than that imposed by W & L (1975), namely $M^{-1} \ll \Phi \ll 1$, and the reasons for it will be given shortly.

In such cases Shercliff (1956) shows that the core flow variables v_x and ϕ are $O(1)$ whilst h and j_z are $O(\Phi)$. In the non-conducting duct the former two quantities were again $O(1)$ but the latter were $O(M^{-1})$, which suggests that the flow here may be analysed in a similar fashion with M replaced by Φ^{-1} throughout. Thus, in a non-uniform region of length $O(1)$ the fluid and current will again move along the surfaces defined by (3.3).

The reasons for the restrictions on the value of Φ stated above can now be given. For the following analysis to be valid it is necessary that the path of least resistance for the current flow to cross the duct (from $z > 0$ to $z < 0$) should be via the fluid over the $O(\Phi^{-\frac{1}{2}})$ length rather than through the walls in a plane transverse to the direction of the mean flow. In terms of the physical constants of the flow this condition may be expressed as

$$\frac{\sigma \times O(a^2)}{O(a\Phi^{-\frac{1}{2}})} \gg \frac{\text{conductivity of wall} \times \text{wall thickness} \times O(a)}{O(a)},$$

which reduces to $\Phi^{\frac{1}{2}} \ll 1$.

In the regions of length $O(\Phi^{-\frac{1}{2}})$ upstream and downstream of the non-uniform region, the leading terms in the expressions for the current density and velocity are still given by (3.5*a–c*) and (3.6*a–c*) and the velocity boundary condition (3.7*a*) still holds. The electrical boundary condition (2.4*c*) may be written here as

$$j_y^{(1)} - j_z^{(1)}f' = -(1+f'^2)^{\frac{1}{2}}\left\{\frac{\partial^2\phi^{(0)}}{\partial z^2} + f'f''\frac{\partial\phi^{(0)}}{\partial z}\right\}, \tag{4.1}$$

where $f(z)$ defines the duct wall. For a circular duct of radius R, $f = (R^2-z^2)^{\frac{1}{2}}$, and after combining (3.5*a–c*), (3.6*a–c*), (3.7*a*) and (4.1) it may be shown that $\phi^{(0)}$ and $h^{(\frac{1}{2})}$ must satisfy

$$(R^2-z^2)\frac{\partial^2 h^{(\frac{1}{2})}}{\partial z^2} - z\left(\frac{\partial h^{(\frac{1}{2})}}{\partial z} + B_y \frac{\partial \phi^{(0)}}{\partial X}\right) = (R^2-z^2)\frac{\partial^2 \phi^{(0)}}{\partial z^2} - z\left(\frac{\partial \phi^{(0)}}{\partial z} + \frac{R}{B_y}\frac{\partial h^{(\frac{1}{2})}}{\partial X}\right) = 0, \quad (4.2a,b)$$

where $X = x\Phi^{\frac{1}{2}}$. (The corresponding equations for a general duct shape are not given because of their cumbersome form.)

As well as satisfying the symmetry conditions (3.9*a*, *b*) and the matching conditions (3.9*g–i*) at $X = 0$, (4.1*a*, *b*) must satisfy the singularity conditions

$$(R^2-z^2)^{\frac{1}{2}}\,\partial h^{(\frac{1}{2})}/\partial z \to 0, \quad (R^2-z^2)^{\frac{1}{2}}\,\partial \phi^{(0)}/\partial z \to 0 \quad \text{as} \quad |z| \to R \qquad (4.3a,b)$$

near the singular regions at $z = R$ and approach the fully developed flow as $|X| \to \infty$, i.e.

$$\phi^{(0)} \to B_y z, \quad h^{(\frac{1}{2})} \to -(B_y^2/R)X + k, \qquad (4.3c,d)$$

where k is a constant whose value in the upstream pipe will be taken as zero.

4.2. *Numerics*

The numerical analysis for the regions of length $O(\Phi^{\frac{1}{2}})$ upstream and downstream of the non-uniform field region closely parallels the analysis presented in §3.4 and the analysis given by W & L (1975) for similar regions in thin-walled pipes upstream and downstream of a thin-walled expansion or contraction. Only the differences between the present analysis and that presented in §3.4 will be discussed here.

Solutions to (4.2*a*, *b*) may be obtained by separation of variables; writing

$$\phi^{(0)} = -R^{\frac{1}{2}}\Phi(\theta)\exp(-\lambda X R^{-\frac{3}{2}}),$$

$$h^{(\frac{1}{2})} = B_y H(\theta)\exp(-\lambda X R^{-\frac{3}{2}}),$$

where $z = R\sin\theta$, results in an eigenvalue problem consisting of the pair of ordinary differential equations

$$\Phi'' = \lambda \sin\theta H, \quad H'' = \lambda \sin\theta \Phi \quad \text{in} \quad -\tfrac{1}{2}\pi < \theta < 0 \qquad (4.4a,b)$$

together with the boundary conditions (4.3), which reduce to

$$H' = \Phi' = 0 \quad \text{at} \quad \theta = -\tfrac{1}{2}\pi, \qquad (4.5a,b)$$

and the symmetry conditions

$$H' = \Phi = 0 \quad \text{at} \quad \theta = 0. \qquad (4.5c,d)$$

Since the forms of (4.4) and (4.5) are identical, addition leads to an equivalent eigenvalue problem consisting of the single ordinary differential equation

$$S'' = \lambda \sin\theta S \quad \text{in} \quad -\tfrac{1}{2}\pi < \theta < \tfrac{1}{2}\pi \qquad (4.6a)$$

together with the conditions

$$S' = 0 \quad \text{at} \quad \theta = \pm\tfrac{1}{2}\pi. \qquad (4.6b)$$

The eigenvalues of the problem (4.6) are the same as those of the problem (4.4) with (4.5), while the H and Φ for the latter problem are given by the even and odd parts of S respectively.

10·6493	870·0496	3104·4867
34·7142	1031·6164	3404·5579
72·5278	1206·9337	3716·3796
124·0918	1396·0014	4042·9518
189·4061	1598·8195	4383·2746
268·4707	1815·3879	4737·3480
361·2857	2045·7068	5105·1721
467·8511	2289·7761	5486·7468
588·1669	2547·5959	5882·0723
722·2330	2819·1661	6291·1486

TABLE 1. First 30 positive eigenvalues for a thin-walled pipe.

Equation (4.6*a*) is a special form of the Mathieu equation, but the tables for Mathieu functions that appear in the literature provide only the first pair of non-zero eigenvalues to problem (4.6) (see W & L 1975). Approximate values of λ can be found by using an eight-term asymptotic expression for large eigenvalues of the Mathieu equation, and the first thirty positive eigenvalues found in this manner are presented by W & L (1975). They conclude that these values are probably quite good since the first approximate value agrees with the correct value to four significant figures. Efforts to use these approximate eigenvalues to generate numerically the eigenfunctions, which are needed to determine the unknown coefficients in the upstream expansions

$$h^{(\frac{1}{2})} = -X + \sum_{j=1}^{60} a_j H_j \exp(\lambda_j X),$$

$$\phi^{(0)} = z + \sum_{j=1}^{60} a_j \Phi_j \exp(\lambda_j X)$$

and in the downstream expansions

$$h^{(\frac{1}{2})} = -B_y^2 X + k + B_y \sum_{j=1}^{60} b_j H_j \exp(-\lambda_j X),$$

$$\phi^{(0)} = B_y z - \sum_{j=1}^{60} b_j \Phi_j \exp(-\lambda_j X),$$

proved futile. Investigation revealed that the numerical integration of (4.6*a*), which generates the eigenfunctions H_j and Φ_j, is extremely sensitive to small changes in λ and that the appropriate eigenvalues given by the eight-term asymptotic expression for large eigenvalues are not sufficiently accurate.

More accurate eigenvalues are obtained for the problem (4.4) with (4.5) by the method used by W & L (1974*a*) for non-conducting ducts. The interval from $-\frac{1}{2}\pi$ to 0 is divided into ten equal segments and (4.4*a*, *b*) are integrated separately for each segment using a fourth-order Runge–Kutta method with various initial conditions for each segment. These integrations give the coefficients in a set of 38 linear equations obtained by equating the values of H, H', Φ and Φ' at the ends of adjacent segments and by satisfying conditions (4.5*c*, *d*). The unknowns in these equations are the values of H and Φ at $\theta = -\frac{1}{2}\pi$ and the values of H, H', Φ and Φ' at $\theta = -0{\cdot}45\pi$, $-0{\cdot}40\pi$, ..., $-0{\cdot}05\pi$. The determinant of the coefficients is zero when a correct eigenvalue has been chosen, so that the value of this determinant serves as an error measure for eigenvalue guesses. An iterative scheme which uses linear interpolation to compute

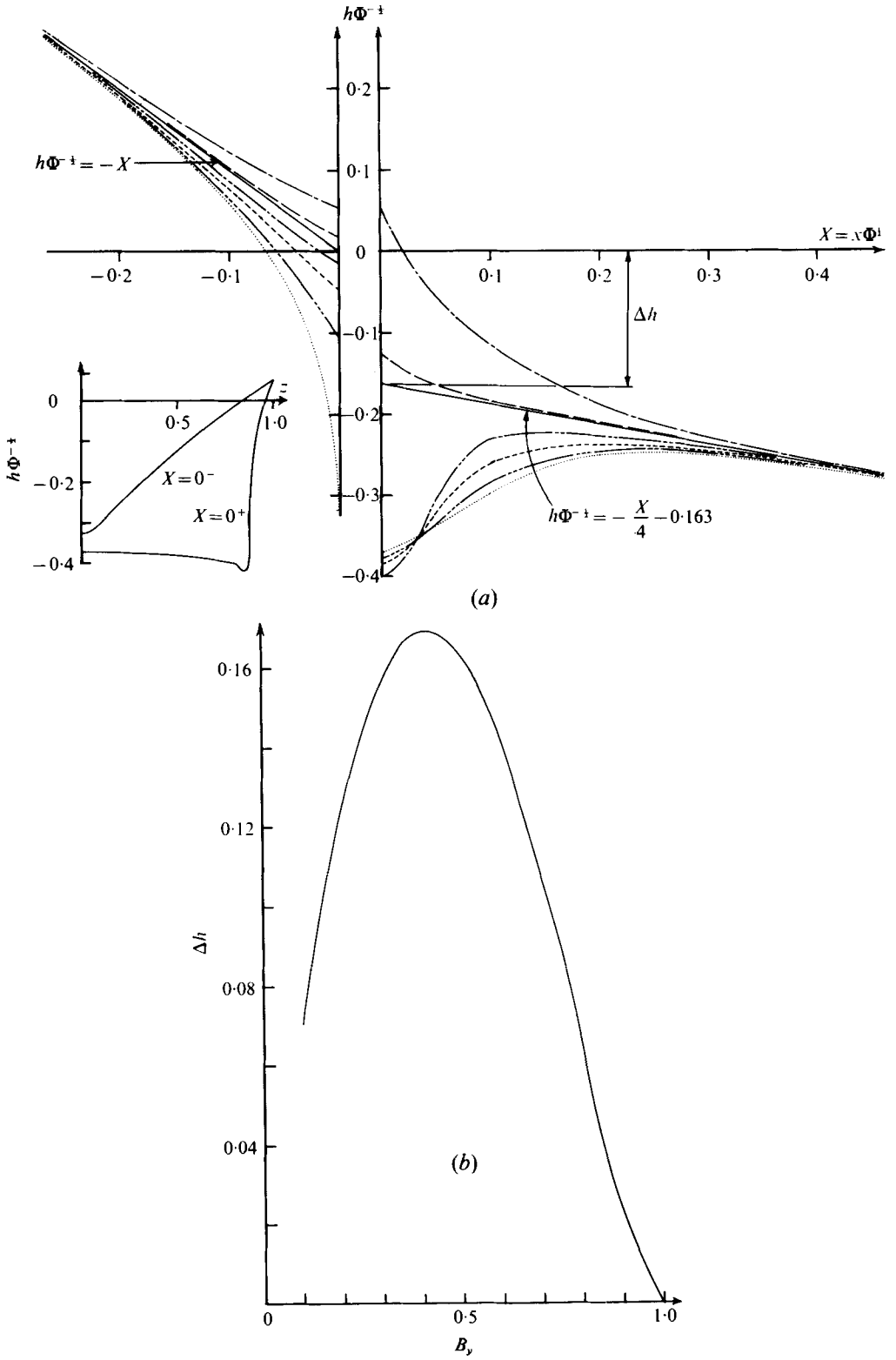

FIGURE 7. (*a*) Pressure distribution along a thin-walled duct on the plane $y = 0$. —·—, $z = 1$; ——, $z = 0{\cdot}9$; —··—, $z = 0{\cdot}8$; – – –, $z = 0{\cdot}7$; —···—, $z = 0{\cdot}55$; ·····, $0 \leqslant z \leqslant 0{\cdot}3$. (*b*) Variation of the pressure drop Δh in a thin-walled duct with B_y.

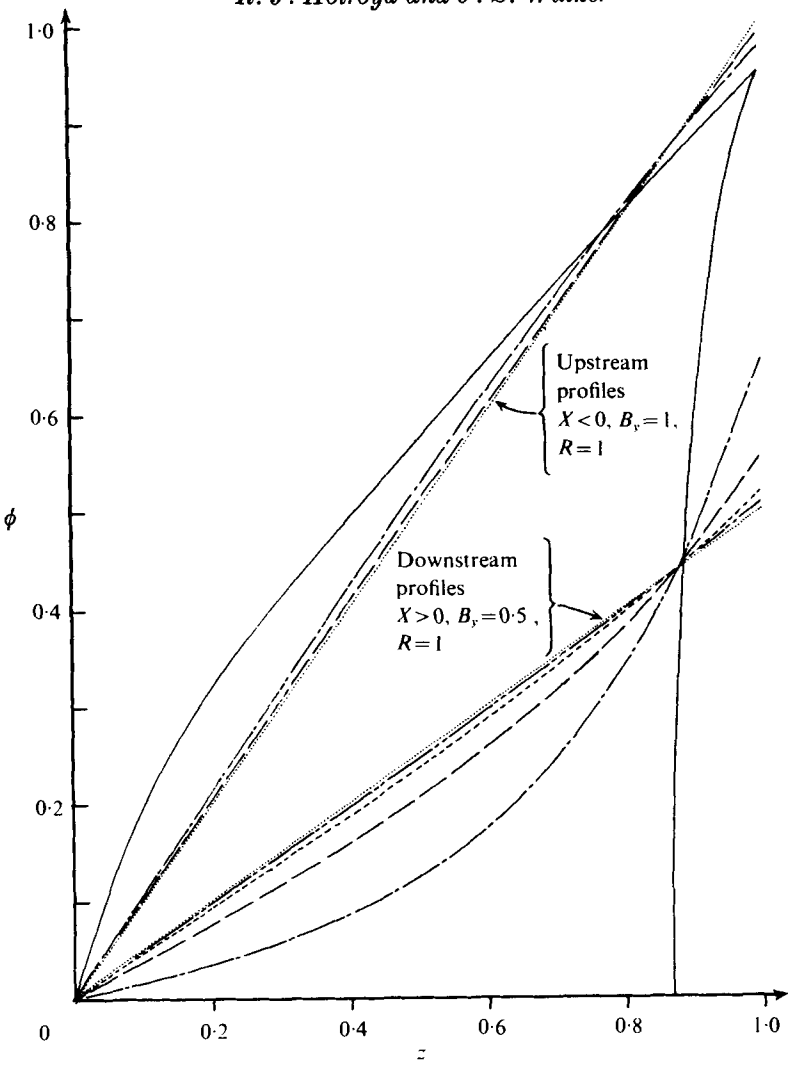

FIGURE 8. Electric potential distribution in a thin-walled duct on the plane $y = 0$. ——, $|X| = 0$; —·—, $|X| = 0{\cdot}1$; — —, $|X| = 0{\cdot}2$; – – –, $|X| = 0{\cdot}3$; — · · —, $|X| = 0{\cdot}4$; · · · · · ·, $|X| \geqslant 0{\cdot}5$.

a new eigenvalue guess based on the two previous guesses with the smallest errors converges to fourteen significant figures within six iterations if it is started from the approximate eigenvalue and a slightly smaller second guess. The first thirty positive eigenvalues are given in table 1.

The remainder of the numerical analysis to determine the coefficients a_j, k and b_j and the values of $\phi^{(0)}$, $v_x^{(0)}$, $h^{(\frac{1}{2})}$, $j_x^{(\frac{1}{2})}$ and $j_z^{(1)}$ at various points (X, z) exactly parallels that given in §3.4 except for minor changes in (3.14a, b). In (3.14a), the integration variable is θ instead of ξ, while the limits of integration for the first and second integrals are $(-\frac{1}{2}\pi, \Theta)$ and $(\Theta, 0)$ respectively, where

$$\Theta = -\arccos\frac{B_y}{R},$$

which replaces (3.14b). Equation (3.9j) again gives Z as a function of z while $z = R\sin\theta$.

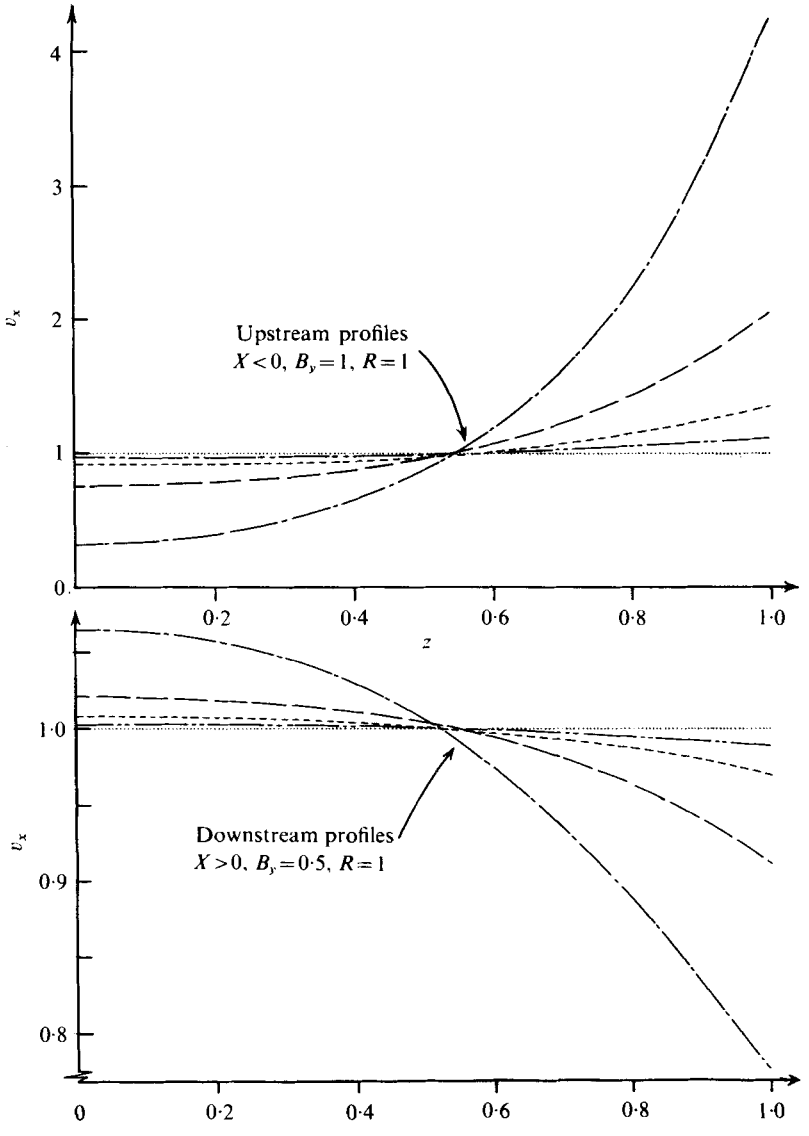

FIGURE 9. Profiles of the velocity component v_x in a thin-walled duct on the plane $y = 0$. Numerical errors preclude computation of profiles at $X = 0^-$ and 0^+. Curves for other values of X as in figure 8.

4.3. *Discussion of computed results for* $B_y = 0{\cdot}5$, $R = 1$

The pressure distribution along the duct and the potential and velocity distributions are shown in figures 7(*a*), 8 and 9 respectively. Qualitatively they vary in much the same way as the corresponding variables in the non-conducting duct.

Again, a pressure drop Δh is introduced into the pressure distribution and its dependence on B_y in a uniform-bore circular duct is shown in figure 7(*b*). Unlike the corresponding pressure drop in the non-conducting duct, which increases as B_y decreases (figure 3*b*), here Δh initially increases and then decreases as B_y decreases.

The reason for this difference lies in the different electrical boundary conditions for the two ducts. Expressed in terms of the streamwise velocity component, for the non-conducting duct (3.7*b*) becomes

$$j_z^{(1)} = -\frac{1}{z}(R^2-z^2)^{\frac{1}{2}}\frac{\partial v_x^{(0)}}{\partial z}$$

and for the thin-walled duct (4.1) becomes

$$j_z^{(1)} = \frac{B_y}{R}\left\{v_x^{(0)} + \frac{1}{z}(R^2-z^2)\frac{\partial v_x^{(0)}}{\partial z}\right\}.$$

In the non-conducting duct the amount of the current associated with the disturbed flow that enters the Hartmann layer depends only on the *vorticity* of the fluid. In the thin-walled duct the amount of the corresponding current that enters the wall is governed by the *velocity and the vorticity* and these terms have opposite signs: a larger positive velocity term implies a larger but negative vorticity term. Thus the size of the pressure drop depends upon the relative magnitude of these two terms.

Considered with the description in § 3.5 of the current flow downstream of the non-uniform region, the fact that less of the disturbance current is needed to satisfy the relevant boundary condition implies that the currents in the walls such as C'' in figure 2, and hence the reverse flow velocities, must be larger than in the non-conducting duct. The fact that even less of the current is syphoned off as B_y decreases points to even larger reverse flows.

5. Final remarks

5.1. *Limitations of the analysis*

Restrictions must be imposed on the values of B_y and R in the downstream part of the duct to ensure that the divided flow in the non-uniform region does not become part of the boundary layers of local width and height $O(R(B_yRM)^{-\frac{1}{3}}) \times O(R(B_yRM)^{-\frac{1}{3}})$ formed where the field lines are tangential to the duct wall (B_yRM is the local Hartmann number). Equation (3.3) implies that the fluid has been squeezed into a region of maximum height B_y by the time it leaves the non-uniform region and so the required condition is

$$B_y \gg R(RB_yM)^{\frac{1}{3}}, \quad \text{i.e.} \quad B_y^2/R \gg M^{-\frac{1}{2}}.$$

In § 2 it was assumed that $M^{-2}|\nabla^2\mathbf{v}| \ll |\mathbf{j}\wedge\mathbf{B}|$ and $N^{-1}|\mathbf{v}.\nabla\mathbf{v}| \ll \mathbf{j}\wedge\mathbf{B}$. Now the velocity gradients throughout the core flow are $O(1)$ in the present approximation even though in the non-uniform region the velocities are larger and the length scale of variations in the velocity is smaller than upstream or downstream of it. Therefore, in a non-conducting duct where $|\mathbf{j}|$ is $O(M^{-\frac{1}{2}})$ at most, the first condition is automatically satisfied and the second one requires

$$N \gg M^{\frac{1}{2}}.$$

In a thin-walled duct where $|\mathbf{j}|$ is $O(\Phi^{\frac{1}{2}})$ the corresponding condition is $N \gg \Phi^{-\frac{1}{2}}$.

5.2. *The effect of increasing the conductance ratio*

Flows along ducts whose conductance ratio Φ has a maximum value restricted by $\Phi^{\frac{1}{2}} \ll 1$ have been examined in this paper. As explained in §4.1, this restriction on Φ ensures that the circulating currents associated with the disturbed flow are confined to the fluid over a long length of the duct rather than flowing through the conducting walls in planes transverse to the duct. It follows that as Φ increases the circulating currents are short circuited via the duct walls. At the same time the transverse core currents increase to a maximum $O(1)$ as $\Phi \to \infty$.

Section 3.5 described how the longitudinal current flow led to a large pressure drop being introduced into the pressure distribution as well as indirectly giving rise to the pair of trapped eddies. As these longitudinal currents are short circuited both phenomena disappear. Furthermore, as the transverse core currents increase to $O(1)$ the pressure gradients increase and the analogy with a perfectly conducting fluid, which led to the derivation of the important equation (3.3), no longer holds. The flow will not then follow the equipotential surfaces in the non-uniform region. It seems likely that as $\Phi \to \infty$ whatever disturbance there is to the flow will be slight and confined to the non-uniform region.

5.3. *Low-N flows*

High-N flows have been studied in this paper for the reasons given in §1. MHD literature does not appear to contain any extensive work on low-N flows for comparison, but some idea of the probable differences in the flows can be obtained from work by Shercliff (1962, §§2.3.1, 3.3.3; 1965, §4.1.4) and Kit *et al.* (1970). Both consider rectangular duct flows with a central region of uniform transverse field flanked by regions of decreasing or zero field and disturbances in the flow invariant in the direction of the field.

For non-conducting ducts their conclusions are similar. An $O(1)$ *circulating current* is set up over an $O(1)$ *length* in the regions of maximum field gradients and these currents lead to *slight* velocity perturbations in the same region, the fluid moving away from the centre of the duct (regardless of its direction of flow). For inviscid flows, Shercliff shows the fractional velocity changes to be $O(\frac{1}{10}N)$ for $N < 2$.

Kit *et al.* retained viscous terms in the equation of motion and obtained solutions by integrating it numerically for two sets of values of M, N and Re, namely 40, 40 and 40 and 63·25, 20 and 200. Their results show that as Re increases, and hence viscous effects decrease, the vorticity created as the flow enters the field is carried downstream and reinforces that created at exit from the field.

In addition, they calculate the flow in a duct where $\Phi \to \infty$ for the first set of M, N and Re values quoted. As in the non-conducting duct a longitudinal current flow is formed but there is very little disturbance to the flow, presumably because the transverse core currents are now more dominant. This part of their work, taken with the statements at the end of §5.2, suggests that as $\Phi \to \infty$ changes in N will have little effect on the flow.

5.4. *Conclusions*

Although two specific problems have been examined at length in this paper, many of the ideas and concepts involved are of a general nature. Only the detailed mathematics would be changed, for example, if the circular duct were replaced by a diamond-shaped

one. Such studies would be of great practical interest, especially for thin-walled ducts, because it has been shown that, for given values of the pressure gradient, conductance ratio and cross-sectional area of a straight duct situated in a uniform transverse magnetic field, the flow rate increases as the duct is elongated in the direction of the field lines (Hunt & Hancox 1971). It is quite possible, therefore, that the pressure drop created by a non-uniform field, for example, might vary with the shape of the duct cross-section.

There are, however, some cases where the present ideas run into difficulties. Consider, for example, two semi-infinite pipes of equal radii in a uniform transverse magnetic field which are offset from each other in a plane parallel to the field and connected by a short pipe of the same radius such that it forms obtuse angles with them. This is simply a variable-area duct problem since when viewed in a direction parallel to the long pipes the cross-section of the connecting pipe is elliptical. Decreasing both angles to 90° produces a singular situation: the flow is squeezed into the boundary layers of the connecting pipe and the problem becomes one of jet flows in a parallel field.

Another problem, perhaps related to that of defining the extent of the non-uniform region (§3.6), is the nature of the velocity profile near the moving fluid/stagnant fluid boundary in the non-uniform region. Numerical problems associated with the truncated eigenfunction solutions preclude computation of velocity profiles in this critical region. J.S.W. believes the velocity gradients to be large yet $O(1)$ while R.J.H. believes that a shear layer of thickness $O(M^{-\frac{1}{2}})$ might separate the moving and stagnant fluid.

The authors would like to thank Dr M. D. Cowley for his constructive comments on earlier drafts of this paper. R.J.H. would like to thank Dr J. C. R. Hunt, who supervised the research work which formed the basis of this paper, for introducing him to J.S.W. R.J.H. acknowledges grants from the Science Research Council and the Culham Laboratory of the United Kingdom Atomic Energy Authority. J.S.W. acknowledges the support of the National Science Foundation under Grant ENG 74-23778.

REFERENCES

HOLROYD, R. J. 1976 MHD duct flows in non-uniform magnetic fields. Ph.D. dissertation, University of Cambridge.

HUNT, J. C. R. & HANCOX, R. 1971 The use of liquid lithium as coolant in a toroidal fusion reactor. Part 1. Calculation of pumping power. *UKAEA Res. Group Rep. Culham Lab.* CLM-R115

HUNT, J. C. R. & HOLROYD, R. J. 1977 Applications of laboratory and theoretical MHD duct flow studies in fusion reactor technology. *UKAEA Res. Group Rep. Culham Lab.* CLM-R 169.

HUNT, J. C. R. & LUDFORD, G. S. S. 1968 Three-dimensional MHD flows with strong transverse magnetic fields. Part 1. Obstacles in a constant area duct. *J. Fluid Mech.* **33**, 693.

KIT, L. G., PETERSON, D. E., PLATNIEKS, I. A. & TSINOBER, A. B. 1970 Investigation of the influence of fringe effects on a MHD flow in a duct with non-conducting walls. *Magnitnaya Gidrodinamika* **6**, 47.

KULIKOVSKII, A. G. 1973 Flows of a conducting liquid in an arbitrary region with a strong magnetic field. *Izv. Akad. Nauk SSSR Mekh. Zhid. i Gaza* **8**, 144.

SHERCLIFF, J. A. 1956 The flow of conducting fluids in circular pipes under transverse magnetic fields. *J. Fluid Mech.* **1**, 644.

SHERCLIFF, J. A. 1962 *The Theory of Electrodynamic Flow Measurement.* Cambridge University Press.

SHERCLIFF, J. A. 1965 *A Textbook of MHD*. Pergamon.

WALKER, J. S. & LUDFORD, G. S. S. 1974*a* MHD flow in insulated circular expansions with strong transverse magnetic fields. *Int. J. Engng Sci.* **12**, 1045.

WALKER, J. S. & LUDFORD, G. S. S. 1974*b* MHD flow in conducting circular expansions with strong transverse magnetic fields. *Int. J. Engng Sci.* **12**, 193.

WALKER, J. S. & LUDFORD, G. S. S. 1975 MHD flow in circular expansions with thin conducting walls. *Int. J. Engng Sci.* **13**, 261.